SPECTRAL ENERGY DISTRIBUTION OF YOUNG STELLAR OBJECTS

Aiswarya Sankar.K[1]*, Mizna Ashraf[2] , Dr. Jessy Jose[2]

[1]Nirmalagiri college, Koothuparamba, Kerala

[2]Indian Institute of Science Education and Research, Tirupati

Project Goals

To determine the evolutionary stage and physical parameters of the young stellar objects in the Dolidze 25 region using SED analysis by utilizing SEDBYS.

What are SED's of YSO's ?

- Young Stellar Objects(YSOs) are stars in early stage of evolution.
- Spectral Energy Distribution is a graph of energy emitted by an object as a function of different wavelengths.
- By analyzing the SED of a YSO, it is possible to uncover the geometry, structure, and constituents of the star.

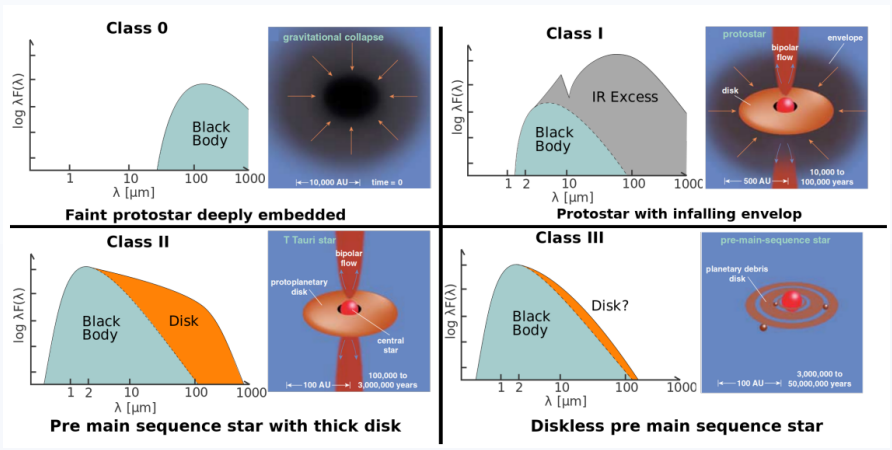

SEDs at different stages of stellar evolution

Image credits : eso.org

Dolidze 25

- Young open cluster associated with the HII region S284.
- Distance ~ 4.5 Kpc : Age ~ 1-2 Myr. (Guarcello et al., 2021)
- Has very low metallicity (~ 1/6 Z_{solar}) (Negueruela et al., 2015).

Optical image of SH2-284 obtained with the 0.9m-meter telescope at Kitt Peak National Observatory, US. The central part of this region is named as Dolidze 25.

Image credits : noirlab.edu

Abstract

Investigating the impact of metallicity on star and planet formation and evolution is crucial in comprehending the conditions in the early universe. In this study, we focus on a metal-poor star-forming region, Dolidze 25, and collect SEDs of the cluster members using the SEDBYS package. The SEDs are then analyzed using the Robitaille SED fitting tool to estimate the physical parameters of the stars.

Methodology

- Collect SEDs of stars in Dolidze 25 using the SEDBYS package.
- **SEDBYS** is a python-based repository for collecting, calibrating and inspecting multi-wavelength photometry and IR spectra (Davies 2021).
- Analyze the collected SEDs using Robitaille 2006 models.
- Obtain physical parameters such as mass, temperature and luminosity from the analysis (Robitaille et al., 2006).

Initial Results and Future Plans

- Used membership list from Guarcello et al., 2021 to identify members of the cluster and obtained SEDs of YSOs in Dolidze 25 using SEDBYS.
- Future plan: Perform Robitaille SED fitting to derive parameters and conduct statistical analysis.

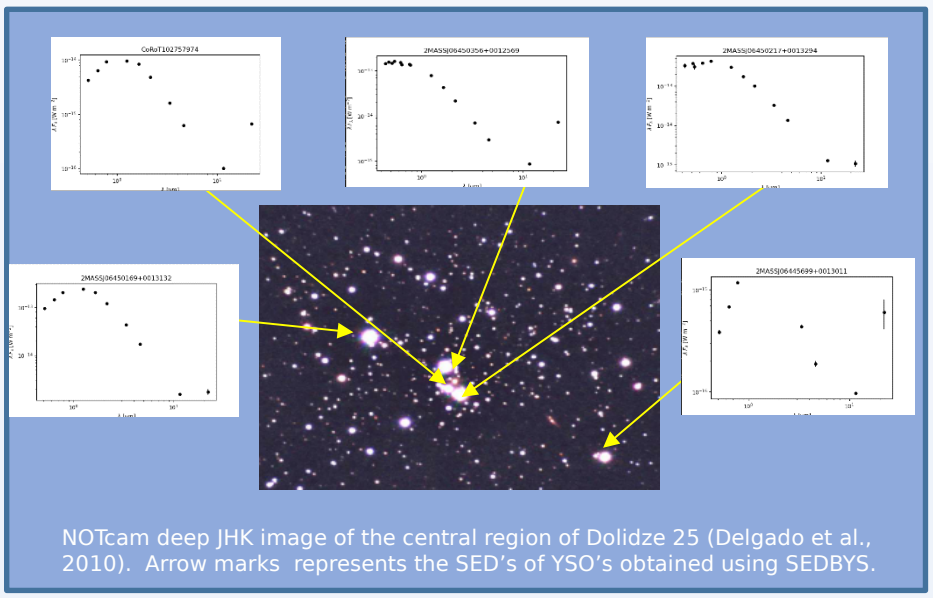

NOTcam deep JHK image of the central region of Dolidze 25 (Delgado et al., 2010). Arrow marks represents the SED's of YSO's obtained using SEDBYS.

References:

1) Davies, Claire L., 2021 SoftwareX 14 : 100687.

2) Guarcello et al., 2021, A&A, 650, 157.

3) Robitaille et al., 2006, ApJ, 167, 256.

4) Delgado et al., 2010, A&A, 509, p.A104.

5) Negueruela et al., 2015, A&A, 584, A77.

* Email: aiswaryasankark@gmail.com

National Seminar on

Advances in Astrophysics & Space Science Research

Determining Filament Counts Using Hydrogen-Alpha Images Of The Sun

Jawahar Raja P[1]

[1]Department of Physics, Dr.N.G.P Arts and Science College, Coimbatore, Tamil Nadu, India

[2]Sun & Solar System Division, Indian Institute of Astrophysics, Bangalore, India

***Corresponding author:** jawaharrajamanjari@gmail.com

Abstract

Filaments are essentially prominences seen as absorbing features on the disk of the Sun. Thus from observations of Filaments taken at Kodaikanal Solar Observatory - Indian Institute of Astrophysics using H – Alpha Telescope the distribution of Filaments over the whole disk image can be studied. For the Solar Cycles 18,19,20 and 21 the Number of Filaments appeared on the Sun is Counted by using Sunspot, Faculae and Prominence Charts available at IIA's Data Archive, I have used 16789 days of data into the analysis. This covers about 50 years. The obtained data are plotted and studied the cyclic behavior of the Filaments appearance on the Sun.

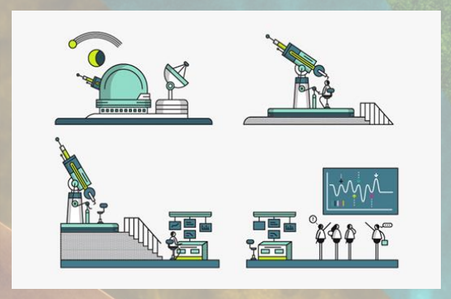

Solar Magnetic Field & Solar Activities

The sun is a magnetic variable star that fluctuates on times scales ranging from a fraction of a second to billions of years. Solar flares, coronal mass ejections, high-speed solar wind, and solar energetic particles are all forms of solar activity. All solar activity is driven by the solar magnetic field.

The magnetic field in this animation is constructed using the Potential Field Source Surface (PFSS) model. The PFSS model is one of the simplest yet realistic models we can explore. Using the solar magnetograms as the 'source surface' of the field, it builds the field structure from the photosphere out to about two solar radii (an altitude of 1 solar radius). These visuals were generated using the Solar Soft package.

In this visualization, the white magnetic field lines are considered 'closed'. The move up, and then returns to the solar surface. The green and violet lines represent field lines that are considered 'open'. Green represents positive magnetic polarity, and violet represents negative polarity. These field lines do not connect back to the Sun but with more distant magnetic fields in space. These field lines act as easy 'roads' for the high-speed solar wind.

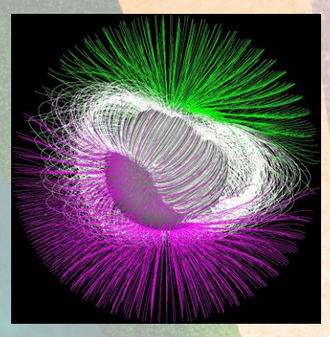

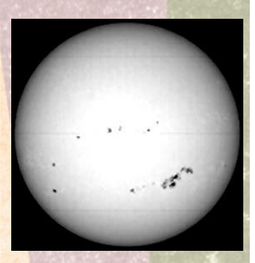

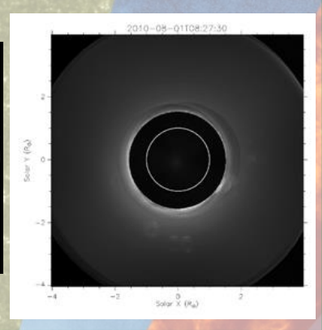

Solar Cycle

Much of the Sun's tempestuous nature comes from its core. At its core is dense, electrically charged gas. Electrically charged gas is a special form of matter called a plasma. This roiling, boiling plasma generates the Sun's powerful magnetic field. Like Earth's magnetic field, the Sun's magnetic field has a north pole and a south pole. On the Sun, however, the magnetic fields are much messier and more disorganized than on Earth.

About every 11 years, the Sun's magnetic field does a flip. In other words, the north pole becomes the south pole, and vice versa.

This flip is one aspect of the roughly 11-year activity cycle the Sun experiences as its magnetic field evolves slowly over time. As the cycle progresses, the Sun's stormy behavior builds to a maximum, and that's when the magnetic field reverses. Then the Sun settles back down to a minimum, only to start another cycle.

Those periods of activity on the sun create what's known as space weather. Solar cycle prediction helps give scientists a rough idea of the frequency of space weather storms of all types, from radio blackouts to geomagnetic storms and solar radiation storms. Space weather can impact the power grid, satellites, GPS and airlines, as well as astronauts and spacecraft.

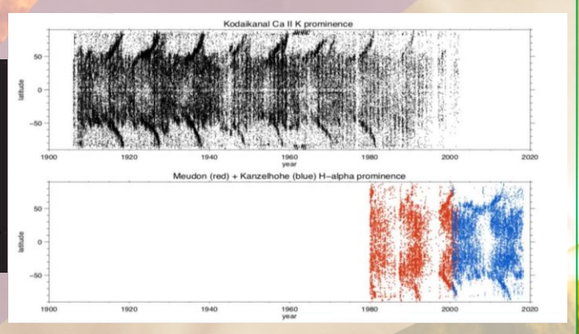

Hydrogen-Alpha Emission

The hydrogen emission spectrum, therefore, consists of several emission lines at different wavelengths throughout the electromagnetic spectrum. Depending on which lower energy state the electron transitions to, they are classified into different series. For example, if the electron from any n>1 state transitions to n=1, the resulting emission spectrum is classified under Lyman series. Similarly, the transition from n>2 to n=2 is classified under Balmer series.

H-alpha (Hα) emission is the red visible spectral line created by a hydrogen atom when an electron falls from the third lowest to second lowest energy level. This transition corresponds to a wavelength of 656.28 nm (red light) and is the first transition in the Balmer series. If we take a look at the Balmer series in the above illustration, you could find that the four spectral lines in the series fall under the visible spectrum, where the red 6563 Å spectral line is Hydrogen-alpha. As hydrogen is the abundant element in the universe, Balmer series plays an important role in spectroscopy and astronomy. The spectral classification of stars depends on it as well.

A hydrogen-alpha filter passes light from the chromosphere in a narrow band around this wavelength while blocking the overwhelming white light that comes through the photosphere. This filtering effect lets you see only glowing hydrogen gas and gives you the contrast to see the Sun for what it really is: a dynamic, seething, and occasionally violent place where immense amounts of energy and hot gas are flung into space over the course of a few minutes or hours.

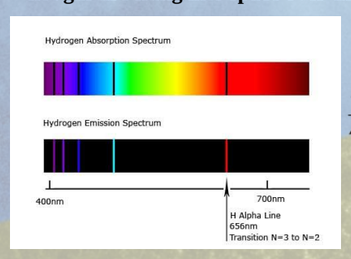

$$\frac{1}{\lambda} = R_H\left(\frac{1}{n_1^2} - \frac{1}{n_2^2}\right)$$

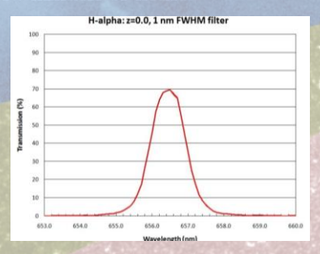

Kodaikanal Solar Observatory

On 20 July 1893 following a famine in Madras Presidency, which underscored the need for a study of the sun to better understand monsoon patterns, a meeting of the U.K. Secretary of State, Indian Observatories Committee, chaired by Lord Kelvin, decided to establish a solar physics observatory at Kodaikanal, based on its southern, dust free, high-altitude location. Michie Smith was selected to be superintendent. Starting in 1895 there was a rapid transfer of work and equipment from the Madras Observatory to Kodaikanal and the observatory was founded on 1 April 1899. The Kodaikanal Solar Observatory is a solar observatory owned and operated by the Indian Institute of Astrophysics. It is on the southern tip of the Palani Hills 4 kilometers (2.5 mi) from Kodaikanal town. From 1902 the solar observations are started sketching and stored in IIA Data archives, there are many solar telescopes and Instruments used at Kodaikanal Solar Observatory.

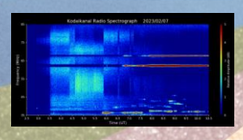

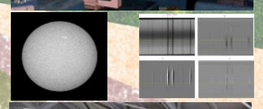

Hydrogen-Alpha Telescope

The H-alpha telescope installed at the Kodaikanal Observatory in October 2014. An objective lens of 20 cm doublet provides f/7.9 beam. With the additional optics, the telescope makes full-disk image of the sun. The telescope is also capable of making magnified view of partial disk of the sun A tunable Lyot filter isolates the H-alpha spectral line. The H-alpha line center image was made with a spectral resolution of 0.4 A. With the 13.5-micron pixel CCD camera the pixel resolution is about 1.21" in full-disk and 0.48" in partial disk mode. The etalon will reject ~90% of the total sunlight but this is not sufficient to provide a safe viewing level so that there will also be an energy rejection filter to bring the light level down to a suitable level. This will also block all the infra-red light which is most damaging to our eyes. Following a further filter to reduce the light intensity placed at the front of the diagonal there is a final 'blocking filter' at the exit of the diagonal which selects only the narrow band centered on the H-alpha line so removing all but the H-alpha emission.

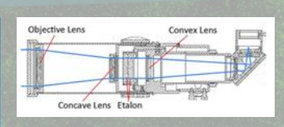

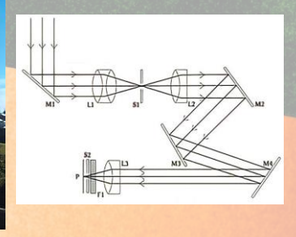

Eruptive Prominences Solar Filaments

A solar prominence (also known as a filament when viewed against the solar disk) is a large, bright feature extending outward from the Sun's surface. Prominences are anchored to the Sun's surface in the photosphere, and extend outwards into the Sun's hot outer atmosphere, called the corona. A prominence forms over timescales of about a day, and stable prominences may persist in the corona for several months, looping hundreds of thousands of miles into space.

The red-glowing looped material is plasma, a hot gas comprised of electrically charged hydrogen and helium. The prominence plasma flows along a tangled and twisted structure of magnetic fields generated by the sun's internal dynamo. An erupting prominence occurs when such a structure becomes unstable and bursts outward, releasing the plasma.

Solar filaments are dark lines or curves that sometimes appear in pictures of the Sun. Filaments are actually huge arcs of plasma (electrified gas) in the Sun's atmosphere. They look dark because they are not as hot as the Sun's surface behind them.

Filaments are held in place by powerful magnetic fields in the Sun's atmosphere. They usually appear above sunspots, which are magnetically disturbed regions on the Sun's surface. Filaments can last for several days - or sometimes up to months! Filaments are most common around the peak of the sunspot cycle (called solar max), the prominences and filaments are well observed using H-alpha imaging telescopes.

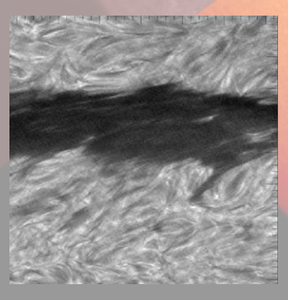

Hydrogen-Alpha Image Observations at KSO

Hα imaging daily observations taken at Kodaikanal Solar Observatory shows Filaments on Sun's photosphere clearly. The observations were sketched and stored in IIA data archives for research use.

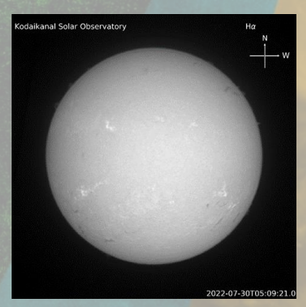

Quiescent Filaments

Quiescent Filaments are filaments that typically Last for 2 or 3 solar rotations.

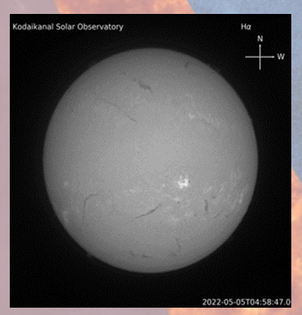

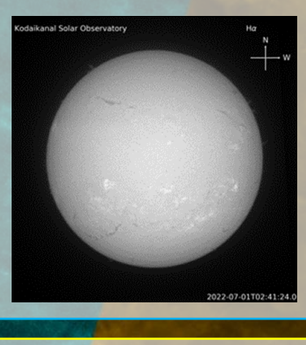

Disparition Brusque

Disparition Brusque are the Active region Filaments that sometimes only appear for few days or Disappear within few hours.

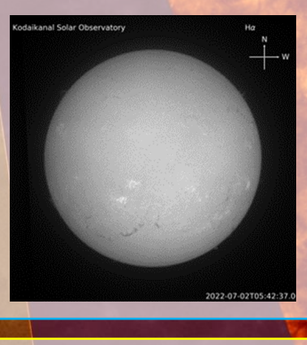

Methodology – Determining Filament Counts

Using Kodaikanal Solar Observatory spectrograph instruments and WARM telescope give full disc images of sun in Calcium K and H-alpha telescope give full disc images of the sun in hydrogen alpha lines are regular use. The two prism K spectrographs were acquired in 1904 and the H alpha grating spectroheliograph was operational in 1911. Since 1912. Prominent pictures over the full limb were obtained in K by blocking the solar disc. The H-alpha images brings positions of filaments over the sun's surface.

The data were sketched on the Sunspot, Faculae and Prominence Sun charts. A sample suncharts has been shown in the figure below. The red lines represent the solar filaments observed on the disk of the sun on that particular day. The green sketching on sunchart represents observations not taken on that day and barrowed data from foreign observatories.

For this project the filaments have been observed on the northern hemisphere and southern hemisphere. KSO has H-alpha data from 1912. This data has translated into sun charts. For this project, sun charts from 1943 have been taken and solar filaments, on a daily basis for the years between 1943 to 1987 has been filaments counted for each hemisphere separately.

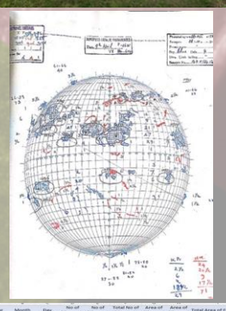

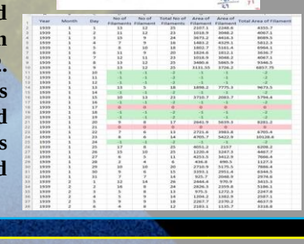

Results & Conclusions

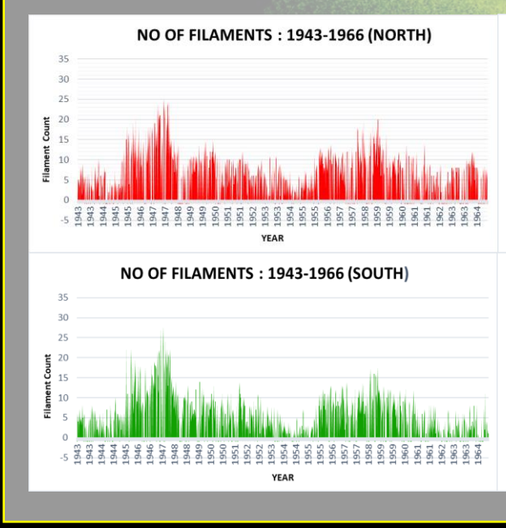

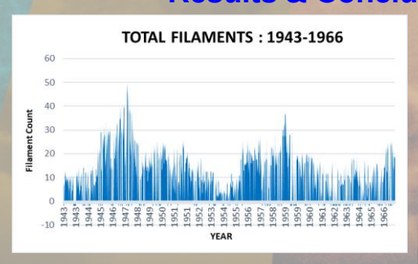

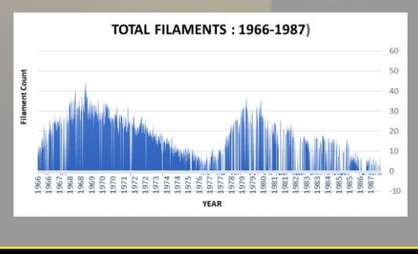

The overall graph chart result shows that total number of Filaments for the solar Cycles 18,19,20 & 21, It covers 16789 days or around 50 years.

The pattern of filaments exhibits almost the same amplitude and their maxima period is also lies very close to sunspot cycle. There we deliver some conclusions from result of the project.

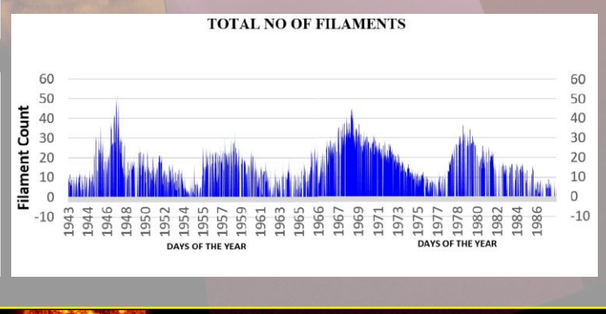

Graph Results Shows Maximum & Minimum Behavior of Solar Filament Counts

- The negative plot values (Green) in the chart are foreign Observatory Observations..
- When the Number of Filaments Increases the Area of Filament also Increases.
- While the data Collection I noted When the days were Filament Counts Increased the plages also Increased.
- Filaments Also have Maxima and Minima during Solar Cycles like Sunspot, Plages, Prominences have maximum & Minimum in Solar Cycles
- Quiescent Filaments and Disparition Brusque Phenomenon were Observed Many Times during project observations.

The study of the Solar Filaments can help us understanding solar magnetic field and the solar dynamo theory also predicting the solar activity for the future cycles, and other solar events such as CMEs to prevent damage of Satellites by solar activities.

Research Guides

Dr. K. GIRIJA
Head of the Department
Department of Physics[1]

Dr. B. Ravindra
Assistant Professor & Head-Sun & Solar System Division
Indian Institute of Astrophysics[2]

Mr. P. Kumaravel
Technical Officer-Observations
Indian Institute of Astrophysics[2]

Highly Thankful to

Dr. Annapurni Subramaniam
Director
Indian Institute of Astrophysics[2]

Dr. E. Ebenezer
Resident Scientist & Head
Kodaikanal Solar Observatory[2]

Reference

Long term Study of the Solar Filaments from the Synoptic maps as Derived from Hα Spectroheliograms of the Kodaikanal Solar Observatory. Subhamoy Chatterjee, Manjunath Hegde, Dipankar Banerjee, and B. Ravindra. The Astrophysical Journal, 849:44 (8pp),2017

Characteristic study of Coronal hole - sunspot interaction

Aswin Amirtha Raj S And Shanmugaraju A

Arul Anandar College(Affiliated to Madurai Kamaraj University),Karumathur,Madurai 625 514

INTRODUCTION

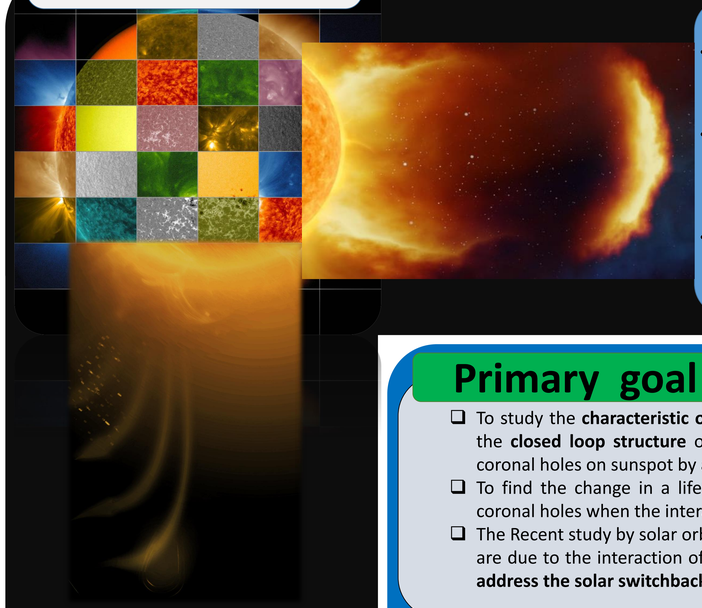

sunspot

- Sunspots are relatively **cool**, **high magnetic**, dark spots on the visible layer of the sun
- The sunspots are always found in pairs with different polarities and are connected by the flux tubes in which plasma flows inside the tube
- These are the **closed-loop magnetic structures** and are the main **source of the solar flares and CMEs**

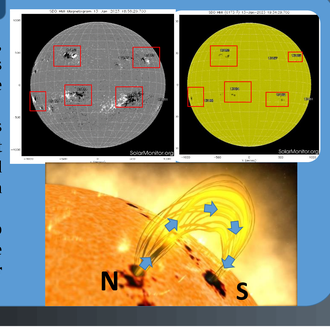

Solar flare

- A solar flare is **an intense burst of radiation** originating from the release of magnetic energy associated with sunspots.
- The flares are mainly **due to Magnetic reconnection** of the magnetic structures of the sunspot
- Solar flares can affect satellite, radio communication, powerlines, and astronauts. it also **acts as an alarm for CME occurrence** hence solar flare prediction is essential for space weather prediction.

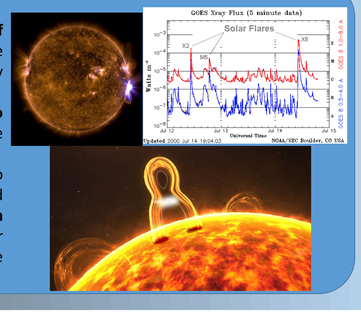

CME

- Coronal mass ejections are large clouds **of solar plasma embedded in the magnetic fields** released into space after solar eruptions and often associated with solar flares.
- These CMEs can travel in the interplanetary medium and interact with the earth's magnetic fields (planets), causing geomagnetic disturbances and can cause space weather effects. Arora is mainly caused due to geoeffective CMEs.
- The average time taken by a CME to reach Earth is about 1 to 3 days, but this can vary depending on various factors

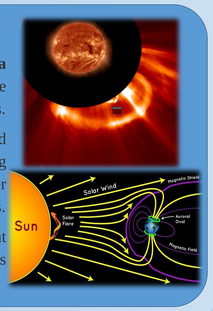

Coronal hole

Coronal holes are regions on the sun's surface where the **corona** is **cooler and less dense**, producing lower brightness and emission levels compared to the surrounding regions.

They are magnetically **open-field line structures** and they are predominantly found in polar regions.

Coronal holes are the main **source of fast solar winds**

The solar wind created by Coronal holes can alter the kinematics of CME and also cause geomagnetic disturbances.

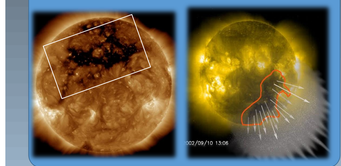

Solar Wind

- Solar winds are **streams of charged particles** (electrons, protons, and heavier ions) **that flow out** from the sun into the solar system at high speeds
- It Travels at speeds of several hundred kilometres per second.
- The solar wind created by Coronal holes can alter CME's kinematics
- The solar **wind speed differs** with respect to **latitude** and **phase of** the **solar cycle**

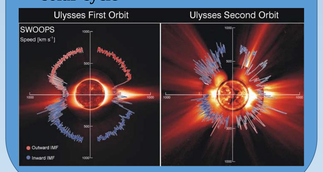

Primary goal

- ❑ To study the **characteristic of open field lines** of coronal holes **interaction** with the **closed loop structure** of sunspot and **study the instability introduced** by coronal holes on sunspot by analyzing the magnetic reconnections(flares)
- ❑ To find the change in a lifetime and the magnetic structure of the spots and coronal holes when the interaction takes place.
- ❑ The Recent study by solar orbiter provides information that the solar switchbacks are due to the interaction of open and closed field structures and this work will **address the solar switchbacks caused due to CH-SS interactions**

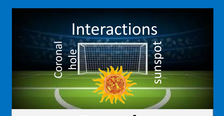

Goals

Secondary goal

- ❑ To **find the change in error for the prediction** of flare using the ML technique when the flaring events with CH-SS interactions are only present in the testing dataset
- ❑ To **compare the F score** of the prediction of flare with both learning and testing data sets containing only Coronal hole nearby spots vs isolated sunspot-originated flares

Data collection

- Using the **Helioviewer** we sort out the events where the Sunspot and coronal holes are in close proximity. And we are finding the similar type of sunspots and coronal holes in the same latitude to compare the properties
- It is desirable to choose the events with isolated sunspot-coronal hole pairs with no nearby sunspots and other magnetic features in solar minima but such an ideal event is nearly impossible or hard to find so some sacrifice is done in the selection process.

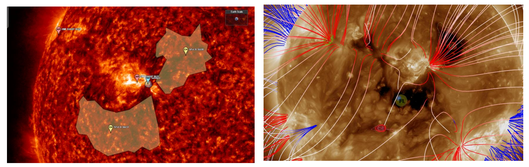

The above fig on the left is an example of a sunspot with a nearby coronal hole view through the helio-viewer. and on the right, we can see the same spot with PFSS magnetic lines extension, and flare due to the CH-SS interactions is also seen.

- sunspot **SHARP data** are obtained from the jsoc website http://jsoc.stanford.edu/doc/data/hmi/sharp/sharp.htm
- The corresponding solar wind speed and plasma density of the coronal holes will be obtained through **Advanced Composition Explorer (ACE)** and High-resolution **IRIS** multiwavelength FITS is utilized to study the flares

Expected Result

✓ We will find the intensity of the **instability** and change in activity introduced by the Coronal holes on the sunspot through the F score and statistical analysis.

Significance: The instability I the magnetic structure can cause the Solar flare and CMEs to form so this instability measure can be useful in predicting the space weather

✓ we can find the relations for SS-CH **interaction rate** with the distance of separation and field strength of Sunspot and Coronal hole pairs.

Significance: This study may lead us to calculate the critical separation distance and field strength and other conditions for CH-SS interaction to occur.

✓ We can see the contribution of the open field line of coronal hole interaction with closed-field sunspot structure in the **solar switchback**

Significance: Used For a better understanding of space weather

✓ If the error of predicting solar flares is more, we can say that the coronal holes can cause a high disturbance in the SHARP parameters(magnetic structures of sunspots).and through the variation in the f-score values of the prediction we may be able to see what are the parameters that get highly altered due to the interaction.

Significance: This may help in improving the prediction of the solar flare by giving weightage for CH-SS interactions in the ML model.

Work Plan

- The first step after successful data collection is to use the **ML technique to find** the **error** in the prediction of flare along **with** their **F scores** for the Sharp parameters of the sunspot with Coronal hole interaction
- Depending on the results from the F score we can indirectly **identify** the **change in SHARP parameters** change due to the SS-CH interaction and give our main focus on those parameters while doing the statistical study.
- **The temporal sequence of the Sunspot area, SHARP parameters** (with high f scores for flare prediction) of the sunspots with nearby Coronal holes are plotted and **compared** with the isolated sunspot plots.
- We wish to **plot the distance of separation** of coronal holes and sunspots **with its activity and chan**ge in the **area** of both Sunspot and coronal holes
- Finally we will **attempt to address the solar switch** back by separating the flare caused due to the **interaction of CH and SS** and **comparing the change in solar wind characters** with respect to the CH-SS interactions.

Difficulties

The **Data collection**: It is the most tedious process in the whole work, especially Finding the isolated sunspot-coronal hole pair with no other magnetic structure nearby is hard Also finding the isolated sunspot and coronal holes of the same type in the same latitude is the next challenge

Flare prediction: Depending on the training dataset and the **ML technique** the **error** may occur so through a change in error we can't get an absolute error correction value for the CH-SS interactions.

SHARP parameters

SHARP stands for Space-Weather HMI Active Region Patches. These data products produced by SDO **contain information about the Sun's magnetic field and active regions**, which can be used to predict the activity of the sunspots. It includes info of Total unsigned magnetic flux ,Mean magnetic field strength, Complexity parameter, Plasma velocity, Entropy index, Sunspot area

all the sunspot have their own SHARP

The study conducted by **Babra et al** used the F-score to identify the most important parameters in predicting solar flares. They **found** that certain parameters, such as **total unsigned magnetic flux, size of the active region, and the sum of the absolute vertical current helicity, were the most important factors in predicting solar flares**.

Solar switchbacks

- Solar switchbacks are **magnetic disturbances in the solar wind** that change direction suddenly and unpredictably.
- They are typically observed in coronal holes and are believed to play a role in the formation and evolution of the solar wind.
- The **formation** of solar switchbacks is thought to be due to a **combination of magnetic reconnection, turbulence, *interplanetary* shocks, and compression regions** in the solar wind. But the mechanical production of the switchback is still a research question

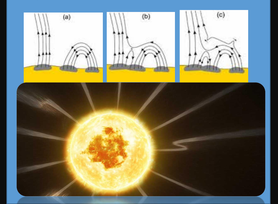

Reference

1. Interaction between Coronal Holes and Active Regions: Evidence from Solar Cycle 23" by Y.-M. Huang, C.-P. Fung, S.-C. Tu, and X.-C. Li.
2. Forecasting Solar Flares Using Machine Learning Techniques: The Application of Random Forest and Artificial Neural Network" by M. B. Babar et al, published in the Journal of Astrophysics and Astronomy in 2015
3. A Comparative Study of Solar Flare Prediction Using Machine Learning Algorithms" by S. J. Chen et al, published in the Journal of Space Weather and Space Climate in 2018.
4. The interaction of coronal holes with active regions and its effect on the solar wind" by L. A. Bale, D. M. Vasquez, T. E. Woods, et al.

ROLE OF COMPUTATIONAL ASTRONOMY IN CALCULATING DYNAMICS OF THE CELESTIAL OBJECTS

Andriya Zenith C P [1 2], Chrisphin Karthick M [3]

[1]Stella Maris College, Chennai, India; [2]Christ (Deemed to be University), Bangalore, India; [3]Indian Institute of Astrophysics, Bangalore, India

ABSTRACT

Observational Astronomy is the study of celestial objects in the universe beyond Earth. This research builds an AstroCalc website for calculating celestial objects' dynamics, primarily focusing on estimating the Julian Date, which is the continuous count of days since the beginning of the Julian period. It also calculates the rising and setting of sidereal rate objects. Also, to finally visualize the celestial objects through a sky map. This work can benefit professional astronomers, amateurs and space enthusiasts to quickly calculate elapsed days between two events and easily point a telescope to the proper coordinates in the night sky. This research is a small step towards achieving the bigger goal for the ephemeris calculations with integrated visualizations. Further can be progressed towards app development.

INTRODUCTION

Astronomy is the study of celestial objects in the universe beyond Earth. All the celestial objects in the sky rise in the east and set in the west. But we know many parameters limit the observation of these celestial objects. Hence, it is essential to locate the celestial objects in the sky. They are into two categories of observations: stars (sidereal rate objects) and nearby solar system bodies (non-sidereal rate objects). This work is done with the help of computational support for the 'n' number of objects in the sky. It focuses on performing calculations regarding sidereal rate objects in the sky by calculating the Julian Date and the Rising and Setting of sidereal rate objects. Also, the website visualizes sidereal rate objects through Aladin Lite. This research is a small step towards achieving the bigger goal for the ephemeris calculations with integrated visualizations.

SYSTEM DESIGN

Julian Date: In this module, the user can convert the calendar date into the Julian date and the Julian date into the calendar date.

Rise and Set: In this module, the user can calculate the rise and set time of sideral rate objects, mainly from the Henry Draper Catalogue (HD), and visually see those objects corresponding to the location of Indian states (for the working sample at different latitudes) and observatories.

Sky Map: In this module, the users can view all celestial objects through the integrated Aladin Lite sky map.

User Guide: The User Guide page is also provided to describe each user page.

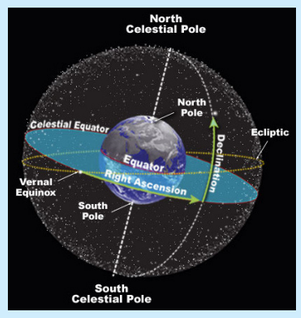

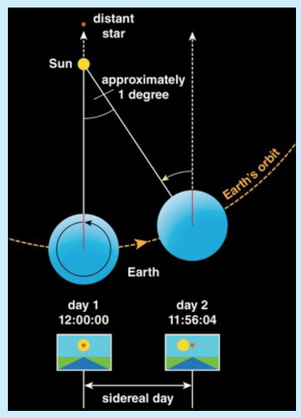

RESULTS

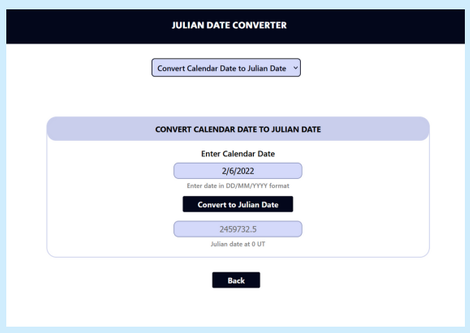

Julian Date Converter

Rise and Set Time Calculator

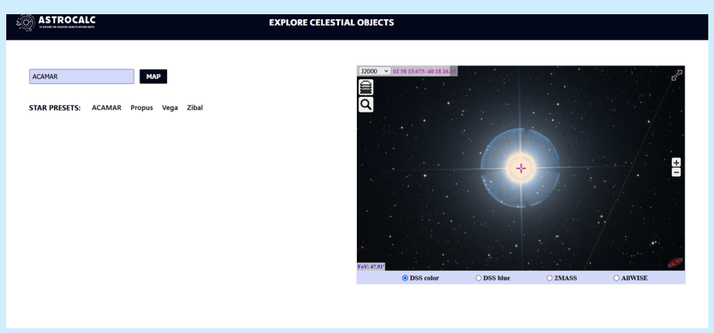

Identifying Celestial Objects

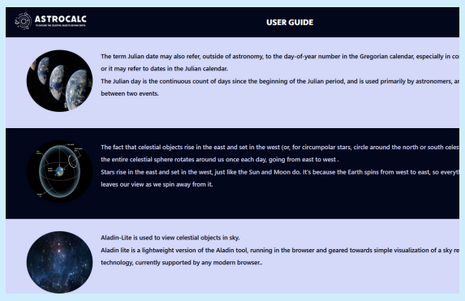

User Guide

CONCLUSION

The project has fulfilled the user's requirements and the admin for calculating astronomical objects and visualizing the objects in the sky. Thus for a given date, calculating the sample of stars as the input varies from 1-24 hours of RA. This application will help to identify the celestial objects in the sky and their availability for observation. Also, this tool will be more helpful for astronomers in observatories and scheduling their observations. It can also be developed to point the telescope and help in observatories' dome rotation and tracking of non-sidereal rate objects. It provides a user-friendly environment where a basic understanding will suffice.

REFERENCES

1. Hannu Karttunen Pekka Kröger Heikki Oja Markku Poutanen Karl Johan Donner. Fundamental Astronomy Sixth Edition, 09 November 2016.
2. Jean Meeus Verniging Voor Sterrenkunda Belgium. Astronomical Formulae for calculators Fourth edition enlarged and revised, October 1, 1988.
3. Peter Duffett-Smith. Practical Astronomy with your calculator, Third edition, August 2012 Print publication year:1989.

andriyazenith05@gmail.com

Finding Features in Galaxy images

Sanjay B

Christ (Deemed To Be University)

National Seminar on Advances in Astrophysics & Space Science Research

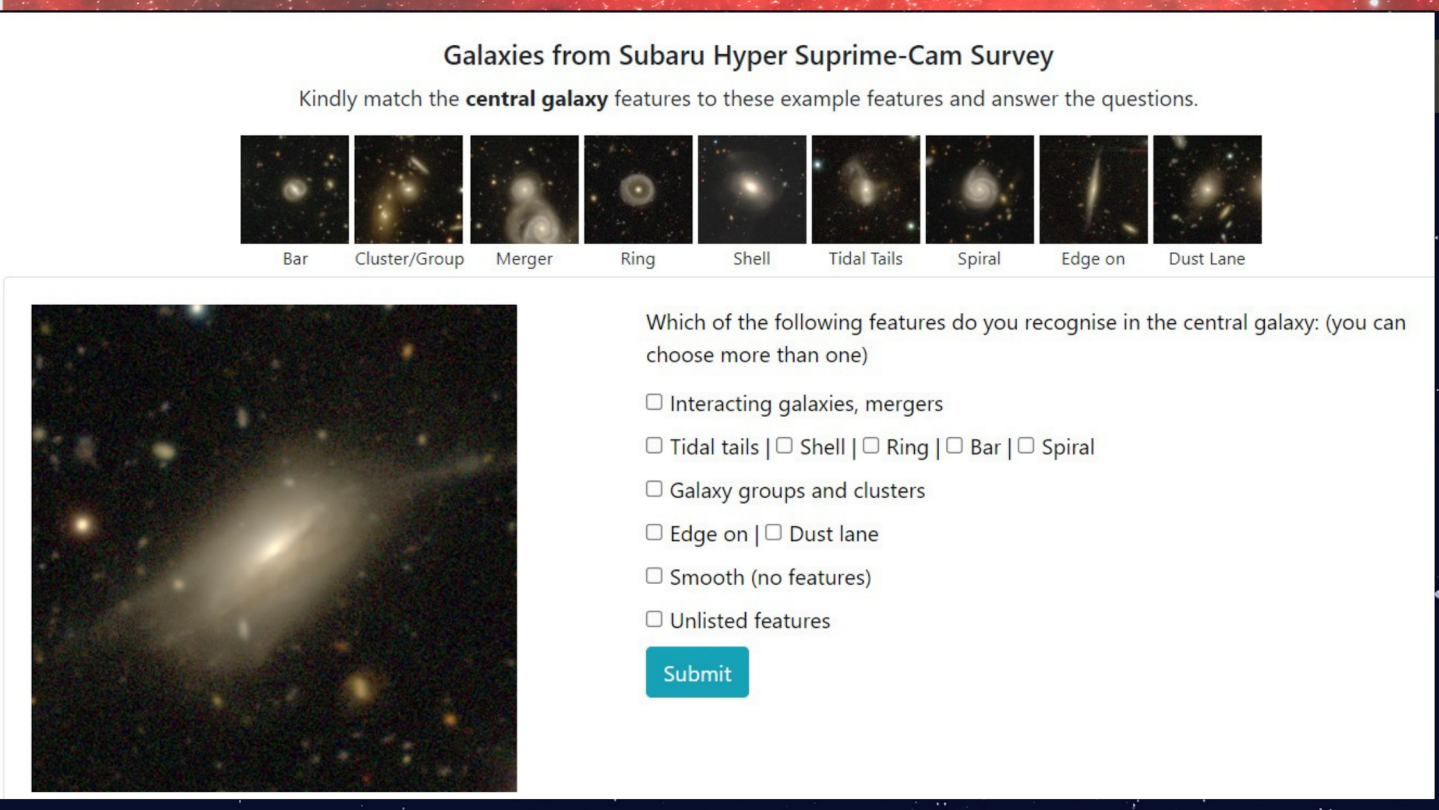

Introduction

Galaxy morphology is a system used for classifying galaxies based on its structural properties. In this work, we identify and understand certain kinds of morphological features in galaxies. We study these features and correlate them with other properties of the galaxies and their environment which helps us in understanding the formation and evolution of galaxies and clusters.

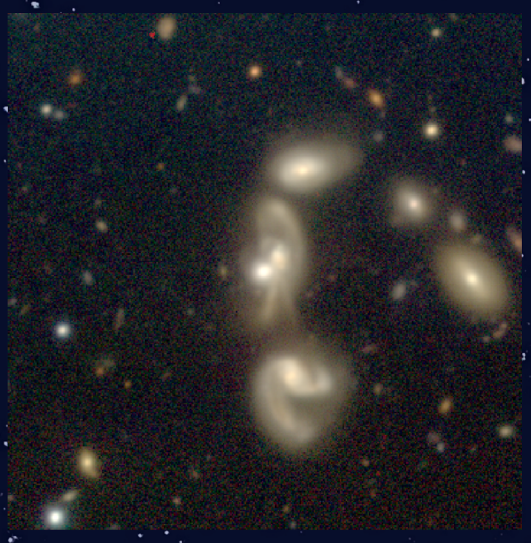

Observations

The data used for the analysis of features in the galaxy images are from Subaru HSC survey which consists of Galaxies discovered by three-layered, multi-band (grizy plus 4 narrow-band filters) imaging survey with the Hyper Suprime-Cam (HSC) on the 8.2m Subaru Telescope. The collective data release includes over 1400 square degrees of the sky.

Methodology and result

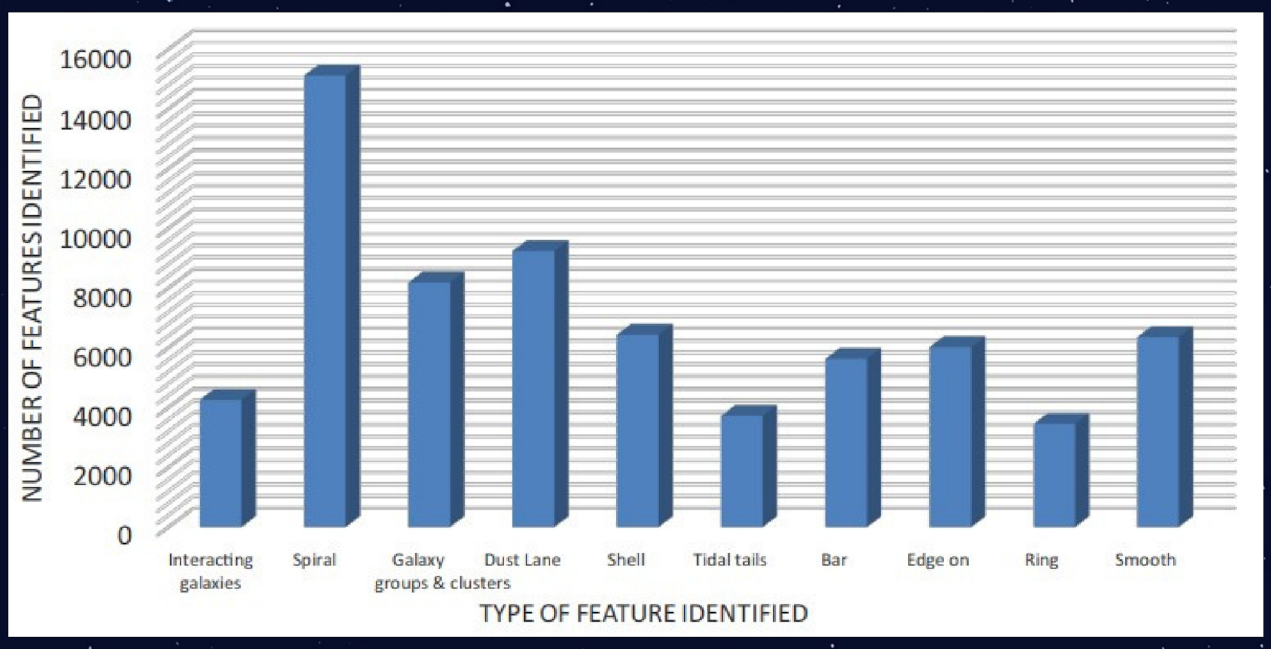

The entire analysis of this project includes around 80,000 features from galaxy images (~1200 citizens) identified until the end of July 2022.

Galaxies are classified based on the structure they look. The features for the classification is mentioned above. If there is some peculiar feature noticed in a galaxy, we list it into an unlisted feature and mentions the details about its peculiarity. If the image observed is flat, we list it into a smooth feature. Out of the 625 galaxy images analysed, 205 images were classified as spiral which also includes 80 images of spiral barred galaxies. Images are regularly added to the database for analysis. Remaining images were classified as (10% - Dust lane; 10% - Galaxy groups and clusters; 16% for shell and edge on galaxies collectively). The project is a part of citizen science program organised by PKC - Pune Knowledge Cluster (Website: https://csa.pkc.org.in/)

References

[1] https://hsc.mtk.nao.ac.jp/ssp/
[2] Aihara et al. 2021. PASJ submitted “Third data release of the Hyper Suprime-Cam Subaru Strategic Program”
[3] https://www.pkc.org.in/wp-content/uploads/2023/01/PKC_Impact-Report_web_090123.pdf
[4] Kawanomoto et al. 2018, PASJ, 70, 66 “Hyper Suprime-Cam: FIlters”

TIDAL INTERACTION: STUDY OF INTERACTING GALAXIES THROUGH DATA FROM NEW AGE INSTRUMENTS

Vidyasagar Bhat[1*], Abirami M[1], Sundar M.N[1], Shanthi N[1]

[1]Department of Physics and Electronics, School of Sciences, JAIN (Deemed-to-be University), Bengaluru, India.

ABSTRACT: *As far as we have observed, the Universe has billions of stars, galaxies which has formed through interaction of the interstellar matter over millions of years. Nearly all of these galaxies, ranging from faint dwarfs to super massive galaxies that shine only in X-rays, to those with beautiful spiral-shaped giants seem to have formed after the big bang. They pervade into the deepest part of space which is being observed by our powerful telescopes. Galaxies are usually separated by huge distances, but sometimes the galaxies tend to interact physically and gravitationally. Such an interaction is called Tidal interaction. These interactions could result in changes in the interacting galaxies at multiple levels. Numerous interacting galaxies have been observed in the Universe. Such interacting galaxies in different phases are studied using photometric and spectroscopic data to understand the influence of the tidal interactions on the morphology, chemical composition, star formation, etc in them. We intend to make use of the latest observational data from facilities like the Hubble Space Telescope, James Web Space Telescope, and Sloan Digital Sky Survey to explore the tidal interactions between interacting/ colliding galaxies.*

TYPES OF GAALXY INTERACTION:

SATELLITE INTERACTION:

Remnants of a minor merger can be observed in the form of a stellar stream falling onto the galaxy NGC 5907. Credit: Hubble, NASA

GALAXY COLLISION:

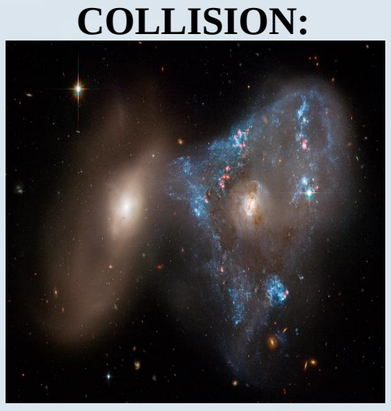

The pair contains the glittery, distorted, star-forming spiral galaxy NGC 2445 at right, along with its less flashy companion, NGC 2444 at left. Credit: Hubble, NASA

GALAXY CANNIBALISM:

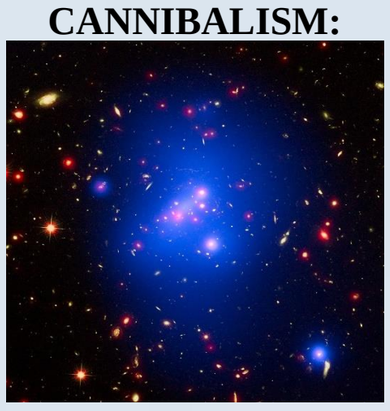

Galaxy cluster IDCS J1426 is located 10 billion light-years from Earth and has the mass of almost 500 trillion suns (multi-wavelength image: X-rays in blue, visible light in green, and infrared light in red).

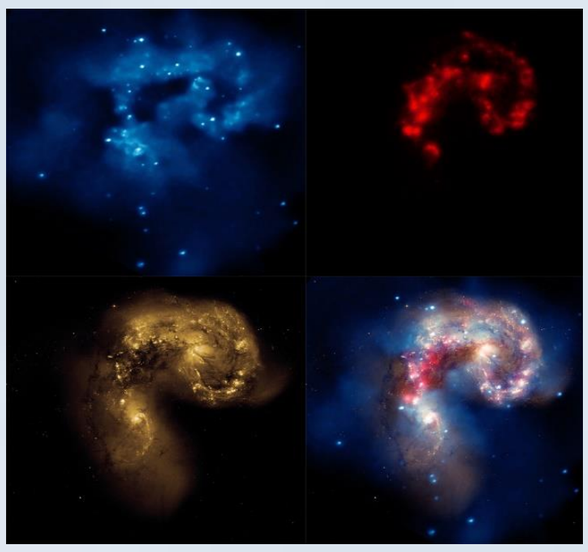

Multi wavelength image of Antennae Galaxy(NGC 4038 and NGC 4039). From top left: X-ray: NASA/CXC/SAO/J.DePasquale IR: NASA/JPL-Caltech Optical: NASA/STScI Right bottom: Composite image

In this computer-generated image, a red oval marks the disk of our Milky Way galaxy and a red dot shows the location of the Sagittarius dwarf galaxy. The yellow circles represent stars that have been ripped from the Sagittarius dwarf and flung far across space. Marion Dierickx / Centre of Astrophysics Harvard and Smithsonian.

STAR FORMATION IN TIDALLY INTERACTING GALAXIES:

When two galaxies come close to each other, the tidal forces between them can compress the gas and dust in each galaxy, leading to the formation of dense regions that are suitable for star formation. This process can lead to an increase in the star formation rate in the interacting galaxies, which can result in the formation of many new stars in a relatively short period of time.

The galaxies also known as NGC 4038 and NGC 4039 are locked in a deadly embrace. Clouds of gas are seen in bright pink and red, surrounding the bright flashes of blue star-forming regions, some of which are partially obscured by dark patches of dust. The rate of star formation is so high that the Antennae Galaxies are said to be in a state of starburst, a period in which all of the gas within the galaxies is being used to form stars. Credit: ESA/Hubble & NASA.

The M82 galaxy experiences gravitational interactions with its galactic neighbour, M81, causing it to have an extraordinarily high rate of star formation, a starburst. Credit: ESA/Hubble & NASA.

METHODOLOGY:

- To find the rate of star formation in the tidally interacting galaxies, we looked at the Arp-Madore Catalogue of Southern Peculiar Galaxies and Associations and Contents.
- There are 25 categories in which several of different classification galaxies are classified on the basis of their type of interaction.
- In those categories two sub categories we have chosen is Elliptical+Spiral and Spiral+Spiral interaction.

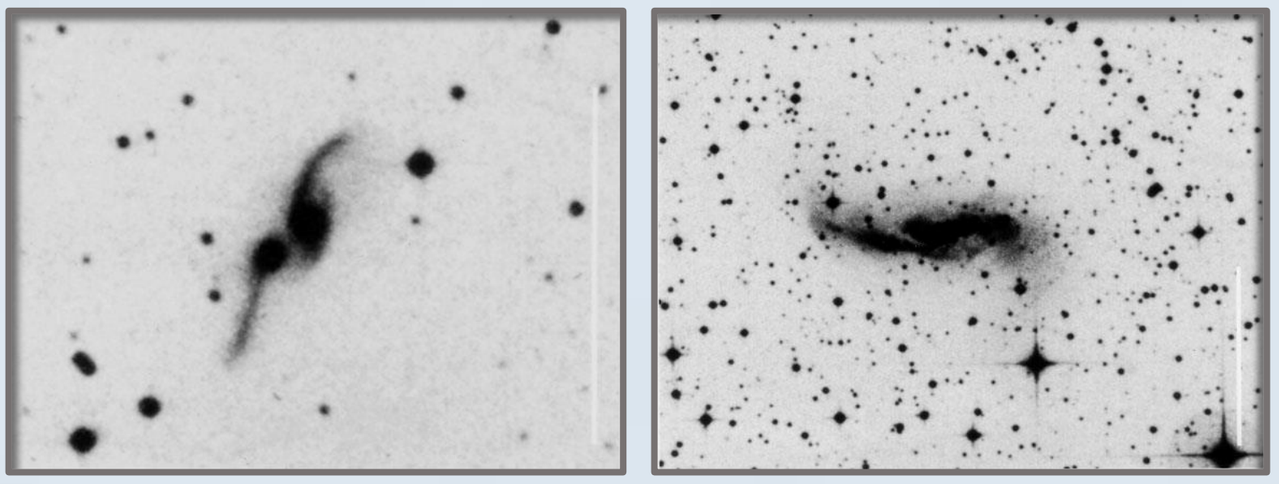

AM2039_242 & AM1007_664 Spirally tidally interacting with each other. Credit Arp-Madore catalogue

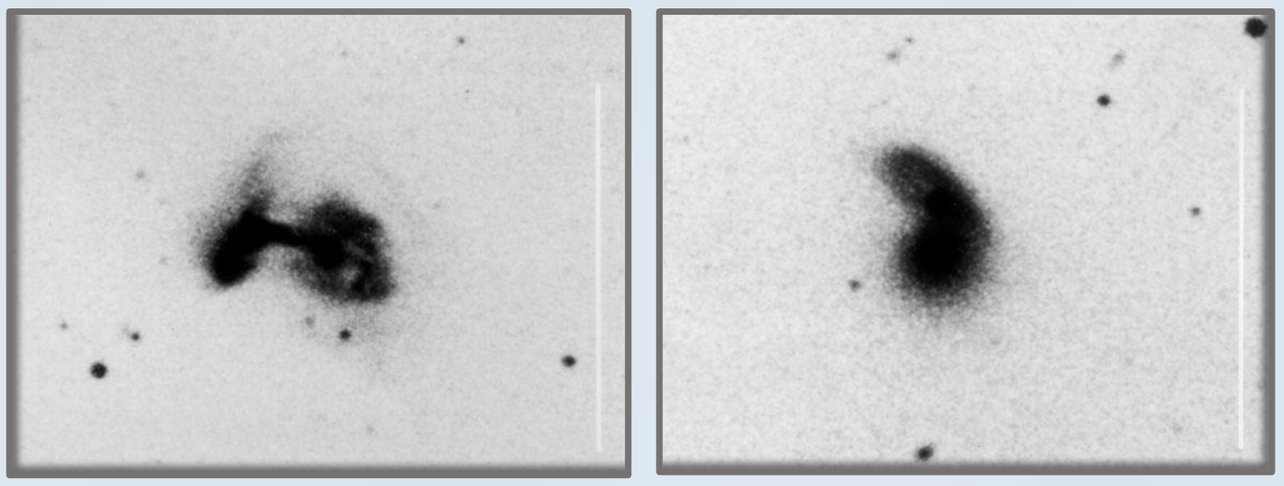

AM1007_664 & AM2353_291 Spiral and Elliptical galaxy tidally interacting with each other. Credit Arp-Madore catalogue

FUTURE WORK:

- Take the spectral data from the chosen E+S and S+S galaxies.
- Use H-alpha line strength to find the star formation rate in the interacting galaxies.
- Compare the SFR's with the average SFR's in Elliptical and Spiral galaxies hence deduce the conclusion.

REFRENCES:

- Di Matteo, T., Springel, V. & Hernquist, L. Energy input from quasars regulates the growth and activity of black holes and their host galaxies. Nature 433, 604–607 (2005).
- Patterson, R., Tidal interaction between a stripped dwarf irregular and elliptical galaxy (1992)
- Di Matteo, T., Concordance between observations and simulations in the evolution of the mass relation between supermassive black holes and their host galaxies (2022)
- Halton C. Arp., A CATALOGUE OF SOUTHERN PECULIAR GALAXIES AND ASSOCIATIONS (1984)

Contact: vidyasagarbhat106@gmail.com

TIMING ANALYSIS OF THERMONUCLEAR X-RAY BURST OF ATOLL SOURCE 4U 1636-536

Riya Fathima K K[1], Juris N J[1], Marykutty James[1], Vishnu Biju[2]
[1]St.Thomas College, Ranni ; [2]Catholicate College, Pathanamthitta

Abstract

In this work we carry out the timing analysis of thermonuclear X-ray bursts from the LMXB 4U 1636-536 using AstroSat/LAXPC data for observations on 02nd February and 09th May 2018. For the two observations, background subtracted light curve in the energy range of 3 to 80 keV is created.
Six thermonuclear X-ray bursts are observed. A long burst with a count rate of ~947 counts/sec and five short bursts with count rate less than 355 counts/sec. A total of 7 dips with approximately 3 seconds of exposure time are observed. For the purpose of examining how burst intensity varies with energy ranges, various burst profiles are created. It is discovered that for all burst profiles, the burst intensity peaks at 3-6 keV and gradually decreases as the energy level rises. The bursts like events are observed only up to 21 keV energy. The model BURS is used to fit the burst-like events. The decay time of the burst profiles is seen to decrease with an increase in energy. Upon analysing the color-color diagram and the hardness-intensity diagram, it was found that the source belonged to the hard spectral state during these observations.

Introduction

4U 1636−536, a persistent X-ray burster, is an LMXB comprising a neutron star and a late-type, low-mass companion star. It is approximately 19.5694 Light Years away with an orbital period of ~3.8 hr and mass of ~1.4 M☉. The companion star is of mass 0.4–0.5 M☉. 4U 1636−536 is classified as an atoll source based on the track it traces in the colour-colour diagram (CCD) and the hardness-intensity diagram (HID) on a ~40-day cycle (Belloni et al,2007).
A thermonuclear X-ray burst (or type-I X-ray burst) is a quick, intense flash of X-ray emission caused by thermonuclear burning occurring on the surface of an accreting neutron star. Due to the intense gravitational pull of the neutron star, when a low-mass main sequence star and companion star are in orbit around one another, the companion star overflows its roche-lobe and hydrogen is dragged into an accretion disc around the neutron star.
This work focuses primarily on doing timing analysis of 4U 1636-536. With the use of specific tools and the softwares like HEASOFT and LAXPC, the AstroSat/LAXPC data of low mass X-ray binary 4U 1636-536 is successfully analysed.

Observation and Data Reduction

The AstroSat LAXPC data for 4U 1636-536 is downloaded from the ISRO Science Data Archive for AstroSat Mission for observations on 02nd February and 09th May, 2018. Further details are given in the table below. The data reduction is done using the software LAXPC developed by IUCAA, Pune.

OBSID	Date of observation	Exposure time (ks)	Burst	Dips
G08_033T 01_900000 1906	02 February 2018	10.43	5	6
G08_033T 01_900000 2084	09 May 2018	10.43	1	1

Timing Analysis

Lightcurves are created for each of these observations. The lightcurve L1 consists of four segments having a persistent count rate of ~200 counts/Sec. The first segment contains a burst B1 with a peak count rate reaching ~360 counts/sec along with two dips D1 and D2. The second and third segments contain two bursts and two dips each. The burst B2 has the second highest count rate of ~351 counts/sec. The dip D3 has the highest negative count rate of ~98.4 counts/sec. The lightcurves are created in 3-5 keV, 5-7 keV and 7-9 keV energy ranges. Since the bursts are short, they are distinguishable only upto 9 keV.

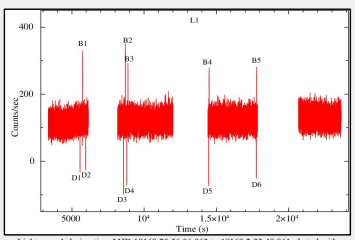

Lightcurve 1 during time MJD 18168 20:56:06:863 to 18169 2:33:48:861 plotted with bin size 1 second in the energy range of 3.0 to 80.0 keV using PCU 2 data.

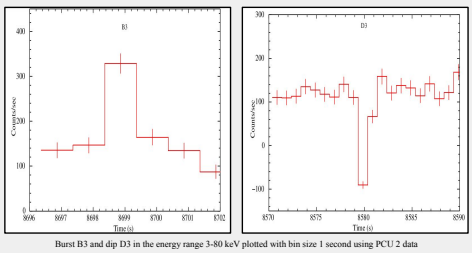

Burst B3 and dip D3 in the energy range 3-80 keV plotted with bin size 1 second using PCU 2 data

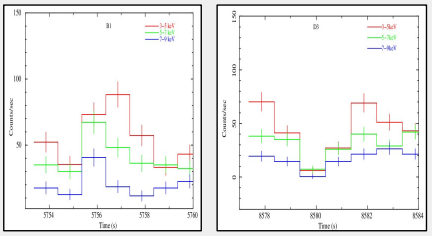

Energy resolved profile of burst B1 and dip D3 plotted for bin size 1 second using PCU 2 data

The lightcurve L2 consists of four segments having a persistent count rate of ~200 counts/Sec. The first segment contains the dip D7 with an exposure time of three seconds. The third segment contains the burst B6 with a peak count rate reaching ~947 counts/sec and decay time of ~7 seconds. The lightcurves in 3-5 keV, 5-7 keV, 7-9 keV, 9-11 keV, 11-13 keV and 13-15 keV ranges are created.

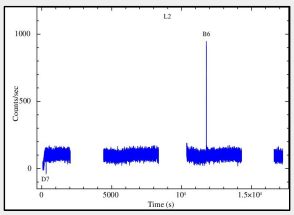

Lightcurve 2 during time MJD 18247 15:01:27:176 to 18247 19:47:00:174 plotted with bin size 1 second in the energy range of 3.0 to 80.0 keV using PCU 2 data

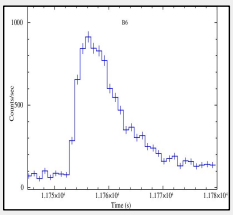

Burst B6 in the energy range 3-80 keV plotted for bin size 1 second using PCU 2 data.

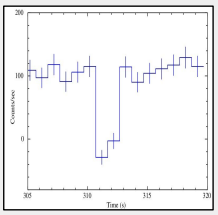

Dip D7 in the energy range 3-80 keV plotted for bin size 1 second using PCU 2 data.

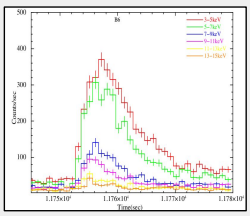

Energy resolved burst profiles of burst B6 plotted for bin size 1 second using PCU 2 data.

To observe the variation of Decay Time with different energies, the individual burst-like events are created in various energy ranges and fitted using model Constant(CO) and BURS. The CO model is used to fit the persistent part and the BURS model to fit the burst region.
The fitted burst profiles of lightcurve 1 in energy ranges 3.0 to 5.0 keV, 5.0 to 7.0 keV, 7.0 to 9.0 keV, 9.0 to 11.0 keV, 11.0 to 13.0 keV and 13.0 to 15.0 keV are shown in the following figures.

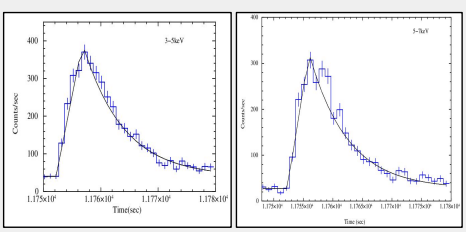

Fitted burst profile of B6 in the 3-5 keV and 5-7 keV energy ranges plotted for bin size 1 second using PCU 2 data.

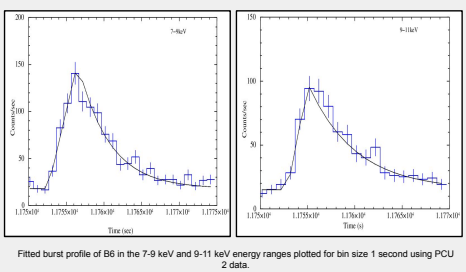

Fitted burst profile of B6 in the 7-9 keV and 9-11 keV energy ranges plotted for bin size 1 second using PCU 2 data.

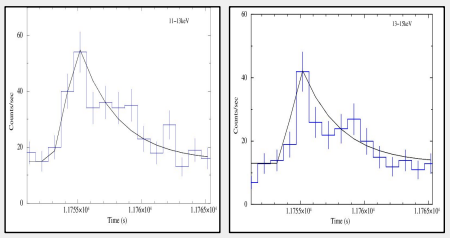

Fitted burst profile of B6 in the 11-13 keV and 13-15 keV energy ranges plotted for bin size 1 second using PCU 2 data.

Decay time versus energy range is plotted.
Hardness intensity ratio of the lightcurves with energy ranges 3 to 6 keV and 6 to 12 keV are created with a binsize of 120 seconds. Y axis represents the Hardness Ratio and the X axis is the total intensity of the lightcurve of energy 3 to 12 keV.
A graph with HR in the Y axis and Time in the X axis is created. The Lightcurves in 3 to 6 keV and 6 to 12 keV are compared with it.
Colour colour diagram is created for the persistent part of the lightcurve with a bin size of 120 s. Lightcurves in energy ranges 3 to 4.5 keV,4.5 to 7 keV,7 to 9.5 keV and 9.5 to 15 keV are created. Y axis is the ratio of the intensity of 9.5 to 15 keV to the 7 to 9.5 keV energy and the X axis is the ratio of the intensity of 4.5 to 7 keV to the 3 to 4.5 keV energy.

Decay time versus energy, hardness ratio versus time, colour colour diagram and hardness intensity diagram are respectively shown in the figures below

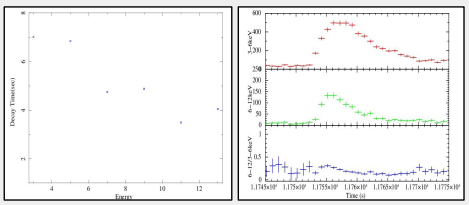

Decay time versus energy and Hardness Ratio versus Time for Lightcurve 2 plotted with bin size 1 second in the energy range of 3.0 to 80.0 keV using PCU 2 data

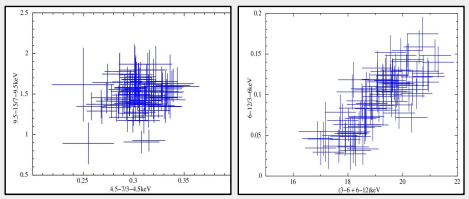

Color Color diagram and Hardness Intensity Diagram of observation 2 plotted with bin size 1 second in the energy range of 3.0 to 80.0 keV using PCU 2 data

Conclusion

- Light Curves in the energy range 3-80 keV were created for the data on 02nd February and 09th May, 2018.
- The light curves shows a total of 6, type-1 thermonuclear x-ray bursts which consists of one long burst, 5 short busts and 7 dips.
- The sixth burst has the highest count rate of ~947 counts/sec.
- The second highest burst has a count rate of ~351 counts/sec.
- The dips shows an exposure time of ~3 sec.
- The highest dip has a negative count rate of ~98.4 counts/ sec.
- Energy resolved analysis of the short bursts shows that the burst-like property is only distinguishable upto 9 keV and for the long burst it is upto 21 keV.
- All of the bursts show a decreasing intensity as the energy ranges are increased. And all the dips shows an increasing intensity as the energy ranges are increased.
- The comparison of the decay time of each burst with different energy ranges showed a similar trait of reduced decay time with increasing energy.
- The source is found to belong to the hard spectral state during these observations, according to the color-color diagram and the hardness-intensity diagram that are created.

References

1. Thermonuclear X-ray bursts in rapid succession in 4U 1636-536 with AstroSat-LAXPC, Beri,Aru; Paul,Biswajit; et all , Monthly Notices of the Royal Astronomical Society, Volume 482, Issue 4, p.4397-4407, 2019.

2. Detection of thermonuclear X-ray bursts and dips from the X-ray binary, Yashpal Bhulla, Jayashree Roy,et all , Research in Astronomy and Astrophysics, Vol. 20 No. 6, 2020 January 10.

3. X-ray Binaries- an overview. M C Ramadevi, January 2007.